

# Amyloid fibrillogenesis of silkmoth chorion protein peptide-analogues via a liquid-crystalline intermediate phase

S.J. Hamodrakas,<sup>a,\*</sup> A. Hoenger,<sup>b</sup> and V.A. Iconomidou<sup>a</sup>

<sup>a</sup> Department of Cell Biology and Biophysics, Faculty of Biology, University of Athens, Athens 157 01, Greece

<sup>b</sup> European Molecular Biology Laboratory, Meyerhofstrasse 1, Postfach 10.2209, D-69117 Heidelberg, Germany

Received 20 June 2003, and in revised form 2 October 2003

## Abstract

Chorion, the major component of silkmoth eggshell, consists of the A and B classes of low-molecular weight structural proteins. Chorion protects the oocyte and the developing embryo from environmental hazards and this is due to the extraordinary physical and chemical properties of its constituent proteins. We have shown previously [FEBS Lett. 479 (2000) 141; 499 (2001) 268] that peptide-analogues of the A and B classes of chorion proteins form amyloid fibrils under a variety of conditions, which led us to propose that silkmoth chorion is a natural, protective amyloid. In this work, we present data showing conclusively that, the first main step of amyloid-like fibrillogenesis of chorion peptides is the formation of nuclei of liquid crystalline nature, which is reminiscent of spider-silk formation. We show that these liquid-crystalline nuclei (spherulites) ‘collapse’/deteriorate to form amyloid fibrils in a spectacular manner, important, it seems, for chorion morphogenesis and amyloid fibrillogenesis in general. The molecular ‘switch’ causing this spectacular transformation is, most probably, a conformational transition to the structure of chorion peptides, from a left-handed parallel  $\beta$ -helix to an antiparallel  $\beta$ -pleated sheet. Apparently, these peptides were suitably designed to play this role, after millions of years of molecular evolution.

© 2003 Elsevier Inc. All rights reserved.

**Keywords:** Amyloids; Fibrillogenesis; Liquid crystals;  $\beta$ -pleated sheet; Electron microscopy; X-ray diffraction; ATR FT-IR; Silkmoth chorion peptides

## 1. Introduction

Amyloidoses are a group of protein misfolding disorders characterized by the accumulation of insoluble fibrillar deposits called amyloids, mostly in extracellular spaces, by self-assembly (Kelly, 1996; Tan and Pepys, 1994). At least 15 different proteins and polypeptides have been identified in amyloid deposits to date (Guijarro et al., 1998; Sunde and Blake, 1998). These include the A $\beta$  peptide in Alzheimer’s disease, the prion protein in the transmissible spongiform encephalopathies, the islet-associated polypeptide in type II diabetes, and other variant, truncated, or missprocessed proteins in the systemic amyloidoses (Kelly, 1996; Tan and Pepys, 1994; Žerovnik, 2002 and references therein). Amyloids consist of amyloid fibrils, which share tinctorial, mor-

phological, and structural characteristics: they bind Congo red, they are seen as uniform (ca. 100 Å unbranched fibrils of indefinite length, which may be straight or slightly curved, and their constituent proteins adopt a ‘cross- $\beta$ ’ structure with the  $\beta$ -strands perpendicular to the fibre axis (Sunde and Blake, 1997; Sunde and Blake, 1998; and references therein).

The phenomenon of the transformation of proteins into amyloid fibrils is of interest, firstly, because it is related to the protein folding problem, and secondly because it is connected to the so-called conformational diseases, the amyloidoses. Consequently, various attempts have been directed towards an understanding of the fibrillogenesis pathway(s), with the aim of developing inhibitors-drugs of therapeutic benefit. These are summarized in several excellent recent reviews (Dobson, 1999; Kelly, 2000; Rochet and Lansbury, 2000; Soto, 2001; Walsh et al., 1999; Žerovnik, 2002). However, the molecular and energetic factors affecting protein

\* Corresponding author. Fax: +30-210-727-4742.

E-mail address: [shamodr@cc.uoa.gr](mailto:shamodr@cc.uoa.gr) (S.J. Hamodrakas).

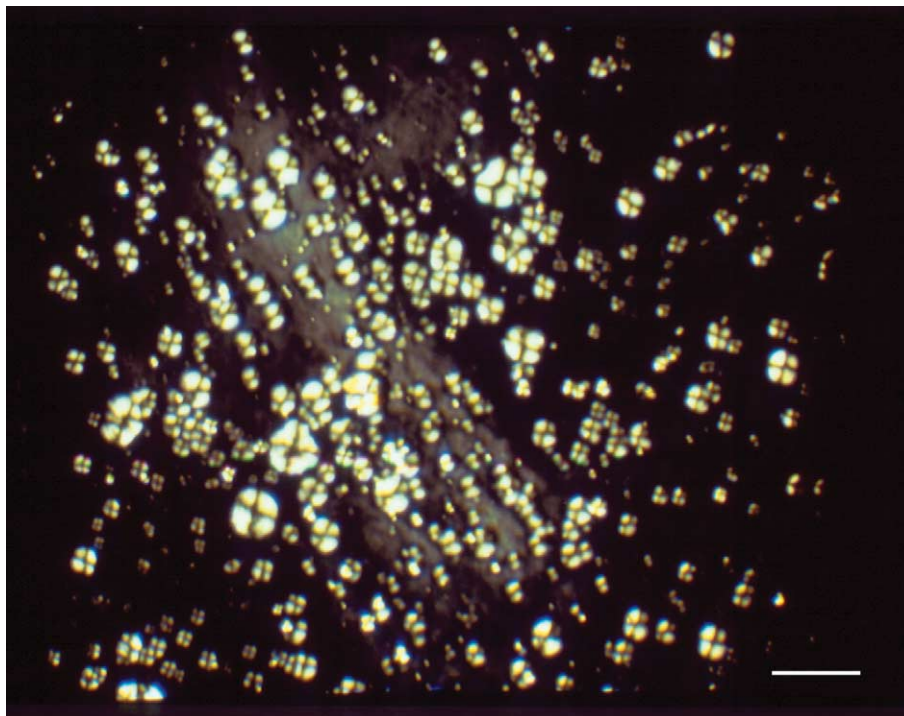


Fig. 2. Photomicrograph of cA peptide spherulites viewed in a polarizing microscope under crossed polars. These supramolecular spherical structures are formed spontaneously after 1–2 h incubation, under a great variety of conditions (see Section 2). ‘Maltese crosses’ are clearly seen. Bar 4  $\mu\text{m}$ .

misfolding and amyloid fibrillogenesis are still largely unknown (Carel and Gooptu, 1998; Soto, 2001).

Chorion is the major component (ca. 95%) of the eggshell of many insect and fish eggs (Hamodrakas, 1992 and references therein). The proteinaceous chorion (more than 95% of its dry mass is protein) is a biological analogue of a cholesteric liquid crystal, a natural helioid. It performs several important physiological functions, mainly protecting the oocyte and the developing embryo from a wide range of environmental hazards (Hamodrakas, 1992 and references therein). In the silkworm, the follicular cells, which surround the oocyte, synthesize, and secrete according to a precise spatial and temporal program, ca. 200 structural proteins onto the surface of the oocyte, which self-assemble to form chorion (Regier and Kafatos, 1985).

Silkworm chorion proteins are variants of two major themes and have been classified into two major classes, A and B (Regier and Kafatos, 1985). Both families of silkworm chorion proteins consist of three domains. The central domain is conserved in both classes and it contains characteristic hexapeptide tandem repeats. The flanking N- and C-terminal domains are more variable and contain also characteristic tandem repeats (Hamodrakas et al., 1985; Hamodrakas, 1992 and references therein). A and B central domains show distant similarities, suggesting that the chorion genes constitute a superfamily derived from a single ancestral gene (Leknidou et al., 1986).

Recently, we have shown that a 51-residue peptide-analogue of the entire central domain of the A family of silkworm chorion proteins (cA peptide, Fig. 1), and, also, an 18-residue peptide-analogue of a part of the central domain of the B family of silkworm chorion proteins (B peptide), form amyloid-like fibrils *in vitro* by self-assembly, under a great variety of conditions (Iconomidou et al., 2000; Iconomidou et al., 2001). These observations, together with structural data collected for silkworm chorion and for its constituent proteins (Hamodrakas, 1992 and references therein), probably suggest that silkworm chorion is a natural, self-assembled amyloid with protective properties, important for the survival and development of the oocyte and the developing embryo (Iconomidou et al., 2000; Iconomidou et al., 2001), in sharp contrast to the ‘destructive’ amyloids responsible for conformational diseases.

In this work, we present data, which clearly show that the first main step of amyloid-like fibrillogenesis from chorion peptides is the formation of liquid crystalline nature. Subsequently, these liquid-crystalline nuclei ‘collapse’ and they are transformed into amyloid-like fibrils in a time-period, which depends on several factors. The transformation is performed, most probably, as a result of a conformational transition to the structure of chorion peptides, from a left-handed parallel  $\beta$ -helix to an antiparallel  $\beta$ -pleated sheet. Chorion peptides, apparently, have been designed to play suitably this role after millions of years of molecular evolution.

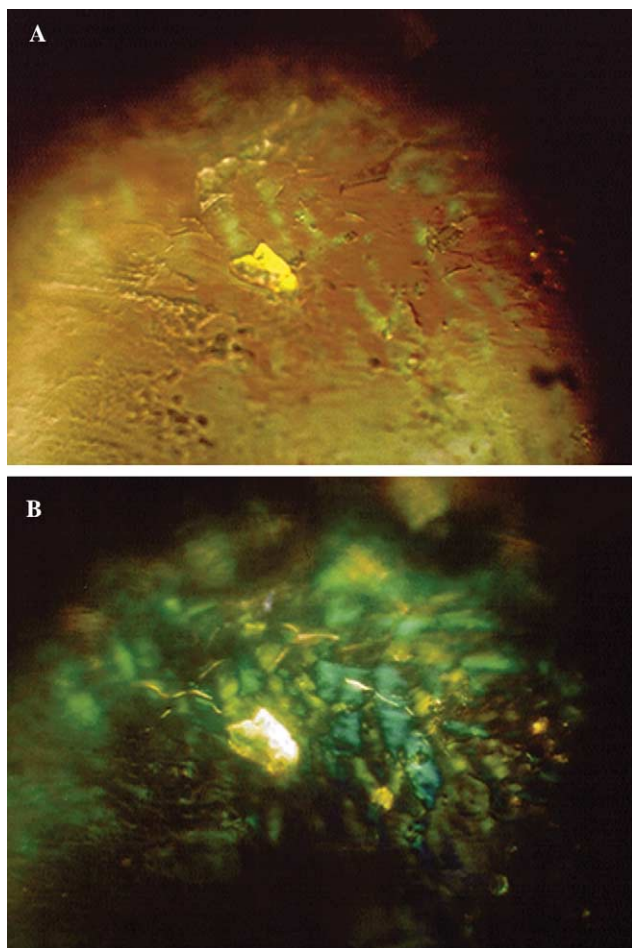


Fig. 10. Photomicrographs of cA peptide fibrils stained with Congo red: (A) Bright field illumination, (B) crossed polars. The yellow–green birefringence characteristic for amyloid fibrils is clearly seen.

This process most probably mimics closely the *in vivo* situation, since silkmoth chorion is a biological analogue of a cholesteric liquid crystal (Hamodrakas, 1992 and references therein).

The data presented in this study support our choice of chorion protein peptide-analogues as model systems to study mechanisms of amyloid-like fibril formation and assembly (Iconomidou et al., 2000; Iconomidou et al., 2001): they provide clues for amyloid formation, which may be important for the design of new drugs in the case of conformational diseases. To our knowledge, this is the first time that a liquid crystalline intermediate is so clearly shown to be involved in the self-assembly mechanisms of amyloid fibrillogenesis.

## 2. Materials and methods

### 2.1. Formation of amyloid-like fibrils

The cA peptide (Fig. 1), synthesized as described by Benaki et al., 1998, was dissolved: (a) in a 50 mM acetate

buffer, pH 5.0, at a concentration of  $6.5 \text{ mg ml}^{-1}$ , (b) in distilled water, pH 5.5, at a concentration of  $6.5 \text{ mg ml}^{-1}$ , (c) in a methanol-distilled water 1:1 mixture, at a concentration of  $6.5 \text{ mg ml}^{-1}$ , and (d) in an ethanol-distilled water 1:1 mixture, at a concentration of  $6.5 \text{ mg ml}^{-1}$ . In all these cases and also in several other cases, varying concentration, temperature, and mixture percentages, it was found to produce gels spontaneously, after 1 week incubation, approximately. These gels contain fibrils, which have tinctorial, morphological, and structural characteristics resembling those of amyloid fibrils (see below). Samples for light and electron microscopy (see below) were collected from the initial solutions, on an every day basis, continuously, for at least 2 weeks.

### 2.2. Negative staining

For negative staining, cA peptide solutions or fibril suspensions were applied to glow-discharged 400-mesh carbon-coated copper grids for 60 s. The grids were flash-washed with ca.  $150 \mu\text{l}$  of distilled water and stained with a drop of 1% (w/v) aqueous uranyl acetate for 45 s. Excess stain was removed by blotting with a filter paper and the grids were air-dried. They were examined in a Philips CM120 Biotwin transmission electron microscope operated at 100 kV. Photographs were obtained with a Gatan 694 retractable slow-scan CCD camera, with a Peltier-cooled chip, mounted at the bottom flange (Gatan, Inc.) utilizing the program Digital Micrograph 2.5.8 (Gatan, Inc.).

### 2.3. Congo red staining and polarized light microscopy

cA peptide fibril suspensions were applied to glass slides and stained with a 10 mM Congo red (Sigma) solution in PBS (pH 7.4) for approximately 2 h. They were then washed several times with 90% ethanol and left to dry. Subsequently, the samples were observed under bright field illumination and between crossed polars, using a Zeiss KL 1500 polarizing stereomicroscope equipped with an MC 80 DX camera.

### 2.4. X-ray diffraction

A  $10 \mu\text{l}$  droplet of peptide cA fibril suspension was placed between two siliconized glass rods, spaced ca. 2 mm apart and mounted horizontally, as collinearly as possible. It was allowed to equilibrate at ambient temperature and humidity for 1/2 h to form a fibre suitable for X-ray diffraction. X-ray diffraction patterns were obtained immediately from these fibres and were recorded on a Mar Research 345 mm image plate, utilizing double-mirror (Prophysics mirror system XRM-216), focused  $\text{CuK}\alpha$  radiation ( $\lambda = 1.5418 \text{ \AA}$ , obtained from a GX-21 rotating anode generator (Elliot-Marconi

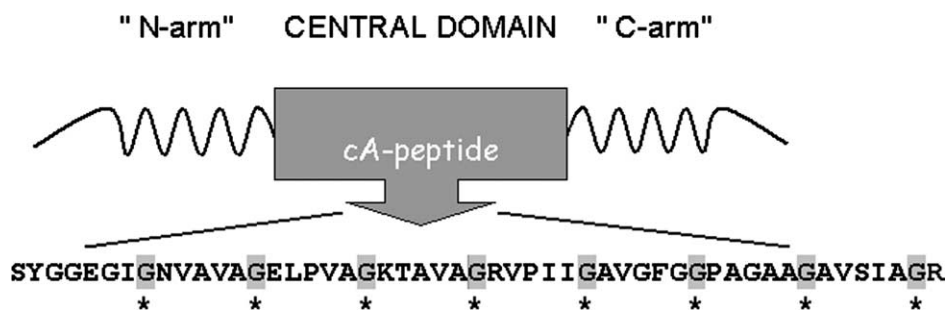


Fig. 1. A schematic representation of the tripartite structure of silkmoth chorion proteins of the A family. A highly conservative central domain of invariant length, and two more variable flanking "arms" constitute each protein. Characteristic, tandemly repeating peptides are present both in the central domain and in the "arms" (Hamodrakas, 1992 and references therein). The amino acid sequence and relative position of the synthetic cA peptide (one letter code), designed to be an analogue of the entire central domain of the A family, is shown. Invariant glycines (G) repeating every six residues are boxed and marked with an asterisk below the sequence.

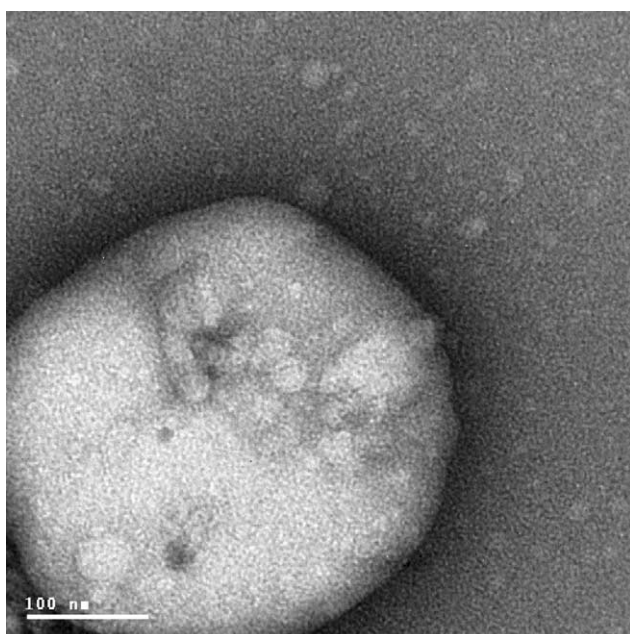


Fig. 3. Electron micrograph of a cA peptide spherulite derived by self-assembly, from a  $6.5 \text{ mg ml}^{-1}$  solution of the cA peptide in distilled water, pH 5.5. The sample was negatively stained with 1% uranyl acetate. Bar 100 nm.

Avionics, Hertfordshire, England) operated at 40 kV, 75 mA. The specimen-to-film distance was set at 150 mm and the exposure time was 30 min. No additional low-angle reflections were observed at longer specimen-to-film distances up to 400 mm. The X-ray patterns, initially viewed using the program MarView (Mar Research, Hamburg, Germany), were displayed and measured with the aid of the program IPDISP of the CCP4 package (Collaborative Computational Project, 1994).

#### 2.5. Attenuated total reflectance infrared spectroscopy (ATR-IR)

A drop of  $10 \mu\text{l}$  suspension of cA peptide fibrils was cast on a front coated Au mirror and was left to dry.

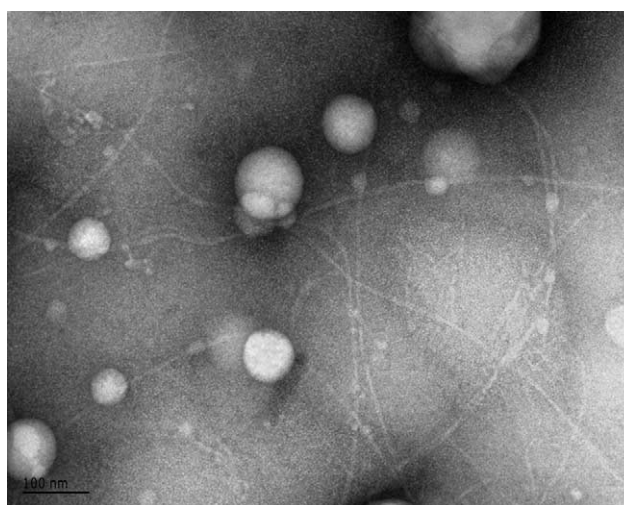


Fig. 4. Electron micrograph of cA peptide spherulites along with readily formed fibrils,  $50\text{--}100 \text{ \AA}$  in thickness, after 1–2 h incubation. The samples were negatively stained with 1% uranyl acetate. Bar 100 nm.

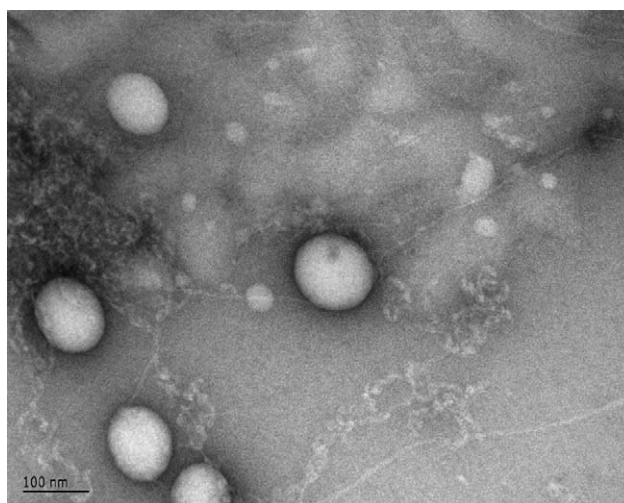


Fig. 5. Electron micrograph of cA peptide spherulites along with readily formed amyloid fibrils, which frequently seem to emanate from spherulites that 'collapse' or 'deteriorate.' The samples were negatively stained with 1% uranyl acetate. Bar 100 nm.

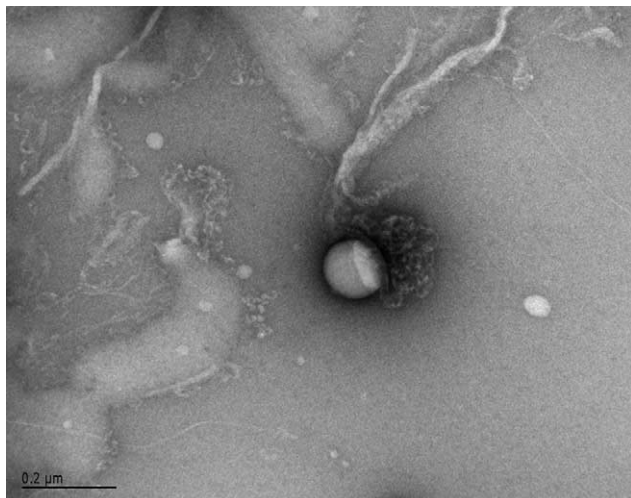


Fig. 6. A ‘snapshot’ of spherulite “collapse”/“deterioration” after 2 days incubation. The sample was negatively stained with 1% uranyl acetate. Bar 0.2  $\mu\text{m}$ .

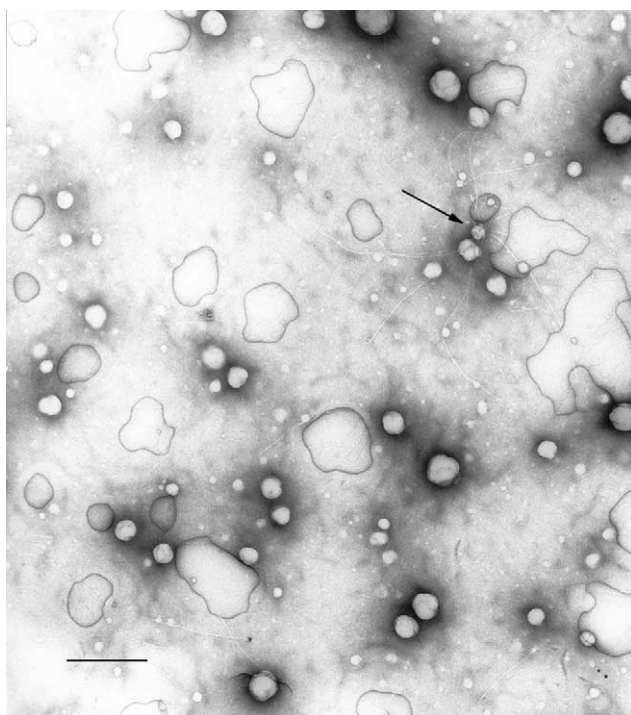


Fig. 7. A ‘snapshot’ whereby multiple fibrils radiate out in all different directions from a “collapsing”/“deteriorating” micelle (arrow), which means that they are derived from the “collapsing”/“deteriorating” micelle. Bar is 400 nm.

Infrared spectra were obtained at a resolution of  $4\text{ cm}^{-1}$ , utilizing an IR microscope (Bruker IRscopeII) equipped with a Ge crystal Attenuated Total Reflectance objective lens ( $20\times$ ), attached to a Fourier-transform instrument (Bruker Equinox 55). Internal reflection spectroscopy presents several advantages compared to the more common KBr dispersion tech-

nique (De Jongh et al., 1996). The choice of the ATR technique was dictated by the need to exclude any possible spectroscopic and chemical interactions between the samples and the dispersing medium. Having a penetration depth of less than  $1\ \mu\text{m}$  ( $1000\text{ cm}^{-1}$ , Ge), ATR is free of saturation effects, which may be present in the transmission spectra of thicker samples. Moreover, the use of an ATR objective lens facilitates the acquisition of data from small samples. Ten 32-scan spectra have been collected and averaged to improve the  $S/N$  ratio. The spectra are corrected for the effect of wavelength on the penetration depth ( $\text{p.d} \propto \lambda$ ). The corresponding effect of the (frequency dependent) refractive index ( $n$ ) of the samples was not taken into account due to the lack of relevant data.

### 2.6. Post-run computations of the spectra

The infrared ATR absorption peak maxima were determined from the minima in the second derivative of the corresponding spectra. Derivatives were computed analytically using routines of the Bruker OPUS/OS2 software and included smoothing by the Savitzky–Golay algorithm over a  $\pm 4\text{ cm}^{-1}$  range, around each data point (Savitsky and Golay, 1964). Smoothing over narrower ranges resulted to a deterioration of the  $S/N$  ratio and did not increase the number of minima that could be determined with confidence.

## 3. Results

cA peptide, an analogue of the entire central domain of the A family of silkworm chorion proteins (Fig. 1), was found to spontaneously assemble into supramolecular spherical structures, after 1–2 h incubation, under a great variety of conditions (see Section 2). These structures, when viewed in a polarizing microscope under crossed polars, are seen to have a liquid crystalline texture. They are spherulites with ‘Maltese crosses’ (Fig. 2). Under a transmission electron microscope, after negative staining, non-transparent spherical structures are seen (Fig. 3), apparently spherulites with smaller diameters (compare with Fig. 2). Spherulites with larger diameters than those shown in Fig. 3 are also seen (not shown). The spherulites appear to have diameters ranging from 0.1 to  $200\ \mu\text{m}$ , combining evidence from light and electron micrographs (Figs. 2 and 3). They frequently coexist with readily formed (after an hour or less incubation) fibrils, 50–100 Å in thickness (Fig. 4). These fibrils frequently seem to be derived from spherulites that ‘collapse’ or ‘deteriorate’ (Figs. 5 and 6). Since it might be argued that the association of spherulites with fibrils is not real, it should be mentioned that upon dilution and re-examination of the samples, fibrils are still seen to coexist with micelle-like structures.

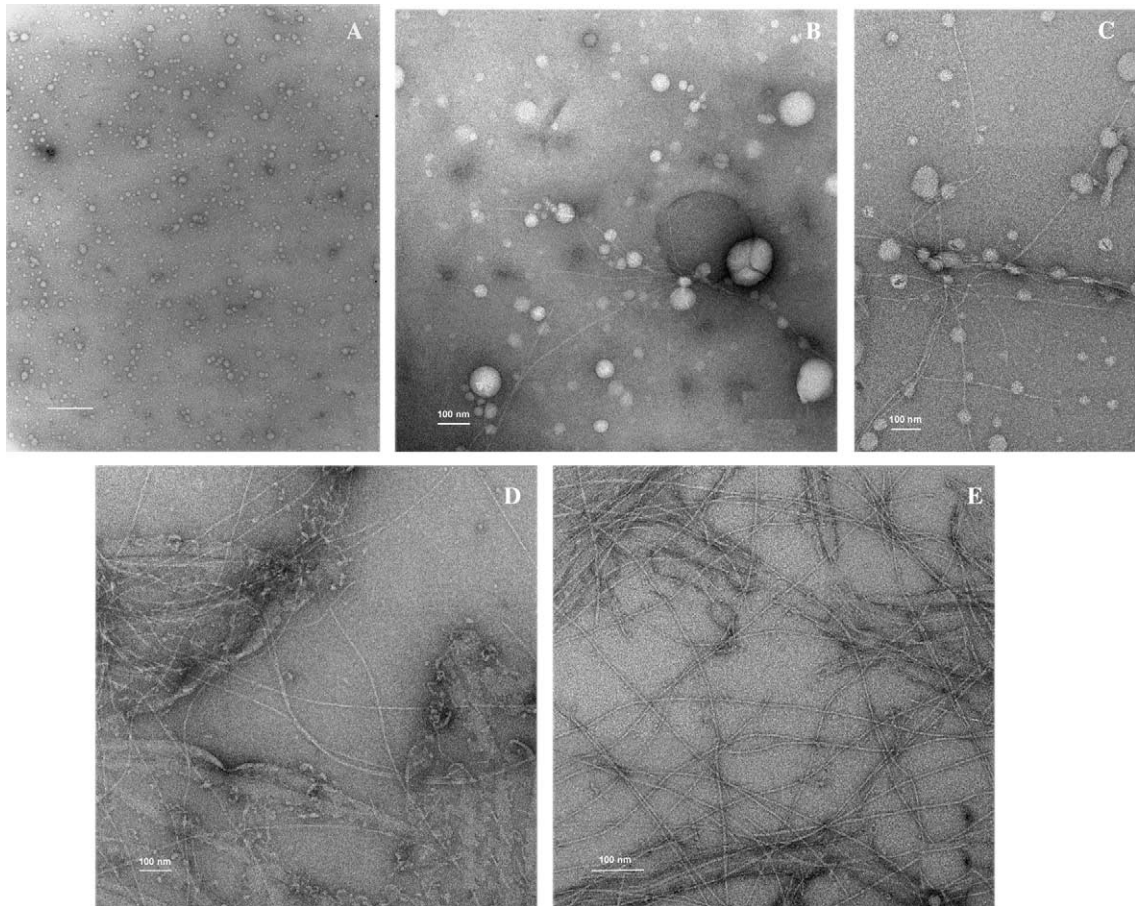


Fig. 8. cA peptide dissolved in a methanol-distilled water 1:1 mixture, at a concentration of  $6.5 \text{ mg ml}^{-1}$  observed for a period of approximately 1 week. It is clearly seen that micelle numbers decrease gradually, with a concomitant increase of straight amyloid-like fibrils. (A) Day 0. Only micelles exist. Bar  $10 \mu\text{m}$  (B) Day 2. Coexistence of micelles with some fibrils. Bar  $100 \text{ nm}$  (C) Day 5. The numbers of fibrils have considerably increased whereas those of micelles decreased. Bar  $100 \text{ nm}$  (D) Day 6. Total disappearance of micelles. The field is full of immature amyloid-like fibrils. Bar  $100 \text{ nm}$  (E) Day 7. Only immature amyloid-like fibrils are seen. Bar  $100 \text{ nm}$ .

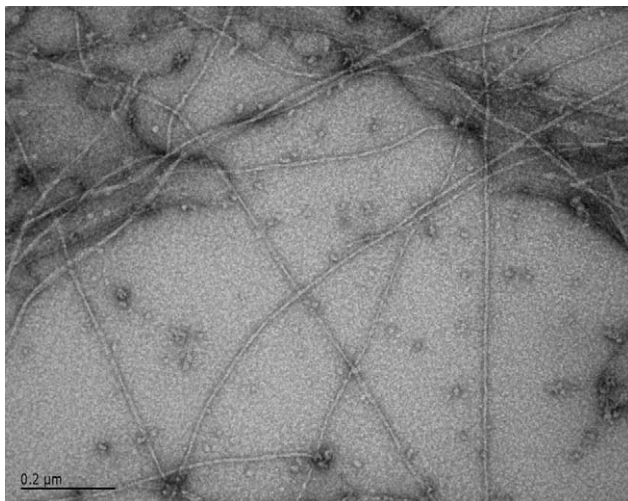


Fig. 9. Electron micrograph of mature cA peptide amyloid-like fibrils, after 1 week of incubation. The sample was negatively stained with 1% uranyl acetate. Bar  $0.2 \mu\text{m}$ .

Furthermore, as seen from Fig. 7, multiple fibrils radiate out from a “collapsing”/“deteriorating” micelle in all different directions, which means that they are indeed derived from the “collapsing”/“deteriorating” micelles. The spherulitic structures are characteristic, (and for the first 2–3 days dominant) features in the electron micrographs, which were taken from the samples, collected from the initial cA peptide incubations, on an every day basis, for approximately 2 weeks. Figs. 8A–E show that in a period of 1 week micelle numbers decrease, with a concomitant increase of straight amyloid-like fibrils. However, quantification is not possible since it appears that there is no obvious statistical relationship between fibrils bound to micelles and free micelles. The exact time of transformation of these spherulitic structures to mature amyloid-like fibrils (Fig. 9) was found to depend mainly on temperature, concentration and type of solution. At room temperature, for the concentrations and types of solutions mentioned in ‘Section 2,’ the time was

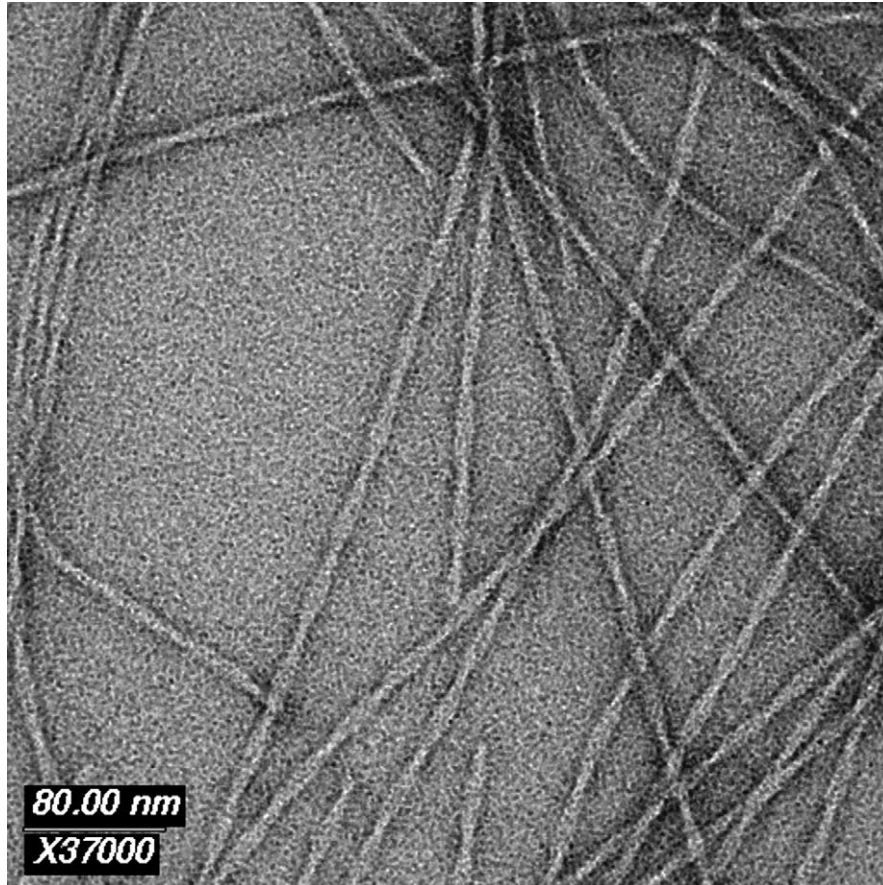


Fig. 11. Electron micrograph of amyloid-like fibrils derived by self-assembly, from a  $6.5 \text{ mg ml}^{-1}$  solution of the cA peptide in a sodium acetate  $50 \text{ mM}$  buffer,  $\text{pH } 5$ . Fibrils are negatively stained with  $1\%$  uranyl acetate. They are of indeterminate length (several microns), unbranched, approximately  $90 \text{ \AA}$  in diameter and have a double helical structure. The pitch of the double helix is ca.  $920 \text{ \AA}$ . A pair of protofilaments each  $30\text{--}40 \text{ \AA}$  in diameter are wound around each other, forming the double-helical fibrils. Bar  $80 \text{ nm}$ .

approximately 1 week. The fibrils formed from the cA peptide solutions exhibit all the hallmarks of amyloids: they bind Congo red showing the characteristic yellow–green birefringence under crossed polars (Fig. 10), they are straight, unbranched fibrils (in fact double-helical fibrils), several microns in length (Fig. 11), and they form oriented fibres giving a characteristic ‘cross- $\beta$ ’ pattern (Fig. 12) (see also Iconomidou et al., 2000). Concomitant evidence that the  $\beta$ -sheet structure of the mature fibrils is antiparallel was also obtained from ATR FT-IR spectra (Fig. 13). In fact, these spectra support the presence of an antiparallel  $\beta$ -pleated sheet structure in the structure of cA peptide (Fig. 13): the strong amide I band at  $1628 \text{ cm}^{-1}$  and the amide III band at  $1234 \text{ cm}^{-1}$  are definitely due to  $\beta$ -sheet (Cai and Singh, 1999; Haris and Chapman, 1995; Jackson and Mantsch, 1995; Krimm and Bandekar, 1986; Surewicz et al., 1993). The high frequency  $1692 \text{ cm}^{-1}$  band (seen as a shoulder in amide I band of the ATR spectrum, Fig. 13) requires special attention. This band is either due to  $\beta$ -turns (joining probably strands of  $\beta$ -sheets, consequently part of the  $\beta$ -sheets themselves) or can be assigned to antiparallel  $\beta$ -sheet. In proteins containing

antiparallel  $\beta$ -sheets, a high frequency  $\beta$ -sheet component that arises from transition dipole coupling is usually found at  $50\text{--}70 \text{ cm}^{-1}$  higher than the main  $\beta$ -sheet component (Jackson and Mantsch, 1995 and references therein). The band at  $1670 \text{ cm}^{-1}$  is a characteristic signature of remnants of TFA, from the isolation procedure of the cA peptide (Benaki et al., 1998).

#### 4. Discussion

The common structural properties of amyloid fibrils most probably imply similar mechanisms of amyloid fibril formation and, perhaps, common features of amyloid disease pathogenesis. Therefore, much effort has been devoted towards understanding the pathway(s) of fibrillogenesis. In the current work it is shown rather conclusively that the first main step of chorion peptide amyloid fibrillogenesis involves the formation of a liquid crystalline phase, immediately after dissolution of chorion peptides in a variety of solvents and environments (Figs. 2, and 3). The spherulitic, liquid crystalline phase formed is preserved for a period of 3–4 days. During this

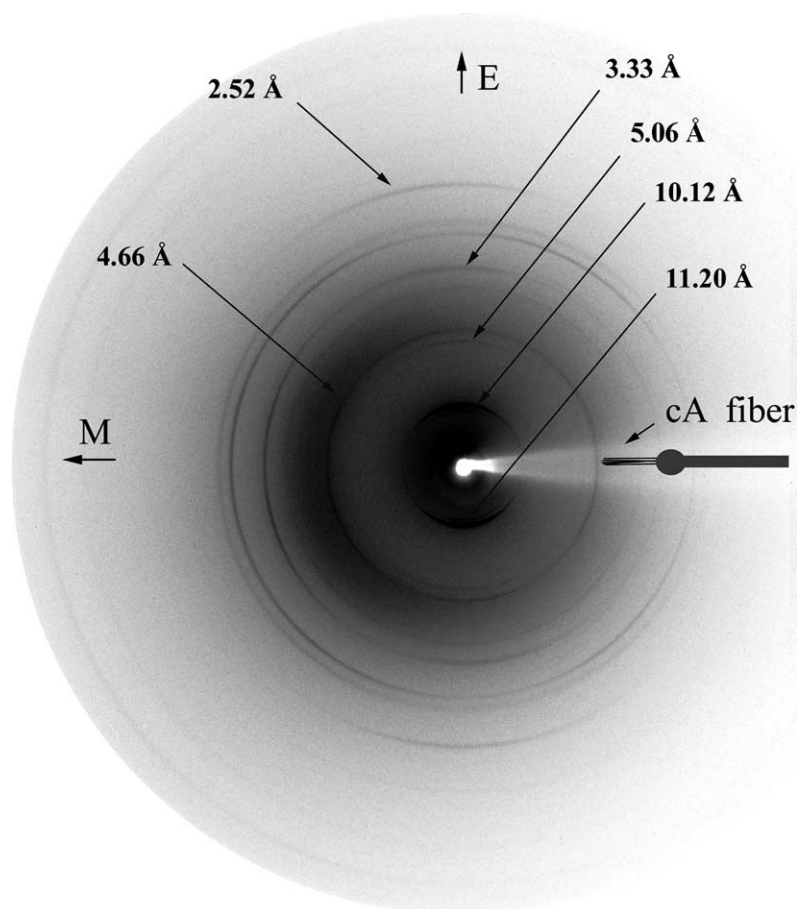


Fig. 12. X-ray diffraction pattern from an oriented fibre of cA peptide amyloid-like fibrils. The meridian, M (direction parallel to the fibre axis) is horizontal and the equator, E, is vertical in this display. The X-ray diffraction pattern is a typical “cross- $\beta$ ” pattern showing a 4.66 Å reflection on the meridian and a 10.12 Å reflection on the equator. This indicates a regular structural repeat of 4.66 Å along the fibre axis (meridian) and a structural spacing of 10.12 Å perpendicular to the fibre axis. The structural repeat of 4.66 Å along the fibre axis corresponds to the spacing of adjacent  $\beta$ -strands (which should be perpendicular to the fibre axis, a “cross- $\beta$ ” structure) and the 10.12 Å spacing parallel to the fibre axis corresponds to the face-to-face separation (packing distance) of the  $\beta$ -sheets. Possible origin and measured spacings of the other reflections have been discussed previously (Iconomidou et al., 2000).

period the spherulites convert gradually into amyloid fibrils in a rather consistent and spectacular manner (Figs. 4–8). They are seen to ‘explode’ producing several short fibrillar components, which, apparently, self-assemble to form long fibrils. Apparently, in previous fibrillogenetic studies of the synthetic amyloid A $\beta$  peptide (Lomakin et al., 1996), micelles of much smaller dimensions (diameters of the order of 140 Å) have been observed to act as initial nuclei from which fibrils emerge. Nevertheless, more recently, the A $\beta$  peptide, at high concentrations of the order of 300–600  $\mu$ M, was found to assemble into clearly defined spheres called “ $\beta$ amy balls,” with diameters of ca. 20–200  $\mu$ m; however, it is not certain whether these spherical structures are spherulites (Westlind-Danielsson and Arnerup, 2001). It is also interesting to note that, AFM images of freshly dissolved A $\beta$  (1–42) peptide after its adsorption onto a freshly cleaned mica surface show predominantly monomeric and dimeric globular structures, with diameters of 1.5–2.5 nm (Parbhu et al., 2002). No fibrillar

structures are observed in AFM images of the freshly dissolved A $\beta$ 's. Repeated AFM imaging reveals that A $\beta$ 's retain the globular and non-fibrillar shape for an extended period of time (Parbhu et al., 2002).

In spiders, soluble proteins are converted to form insoluble silk fibres, stronger than steel and, recently, the amyloidogenic nature of spider silk has been documented (Kenney et al., 2002). An important lesson to learn from the spider is how it stores protein molecules in a highly concentrated liquid crystalline state and then extends these in the spinning duct to form a supremely tough thread (Vollrath and Knight, 2001). Apparently, this is another clear case where formation of insoluble, very tough material with amyloidogenic properties, initially passes through a liquid crystalline state. Observing closely both cases, the transformation of liquid crystalline soluble spider silk into fibres stronger than steel and also the transformation of soluble silkmoth chorion proteins into silkmoth chorion, a structure with extraordinary mechanical and thermal properties, via a

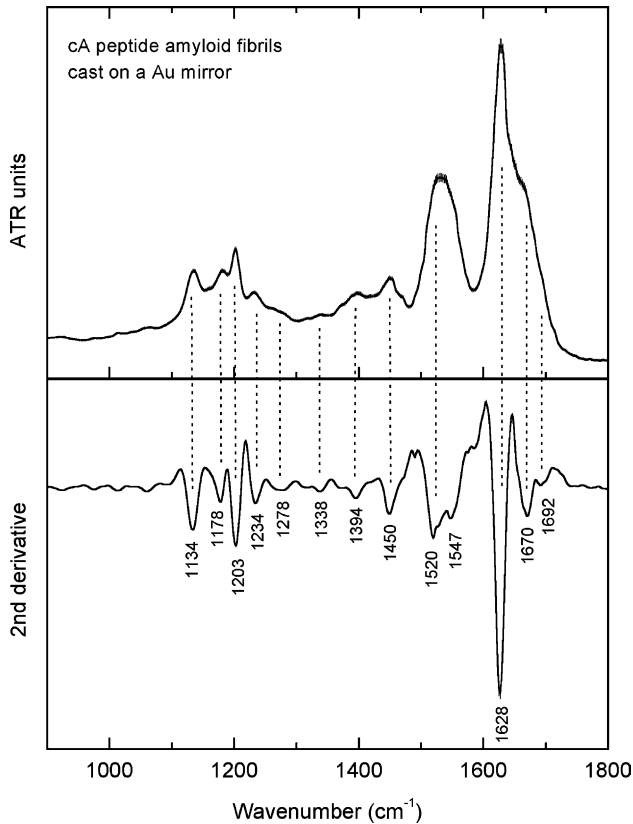


Fig. 13. ATR FT-IR (900–1800  $\text{cm}^{-1}$ ) spectrum of cA peptide amyloid fibrils, cast on a Au mirror. Second derivative spectra are included. Errorbar equals  $\sigma$  in the IR spectrum.

liquid crystalline phase, may help us to gain insight, through lateral thinking, into the sudden but unwanted assembly of other proteins into amyloids, in various amyloidoses.

At this stage, it is obviously natural to wonder what is the molecular denominator of the spherulitic and of the mature fibrillar state. The view that is currently valid is that amyloid fibrillogenesis requires partial unfolding of globular proteins or partial folding of disordered proteins (Rochet and Lansbury, 2000). However, in the case of the cA chorion peptide none of the above views may necessarily be true. Apparently, when cA adopts its final structure forming mature amyloid fibrils it has a characteristic antiparallel  $\beta$ -pleated sheet structure strongly supported by X-ray diffraction, ATR FT-IR, FT-Raman spectroscopy and modelling data (Iconomidou et al., 2000 and Figs. 12 and 13 of this work) and this is obviously its dominant molecular structure in the amyloid fibrillar state. It is tempting to speculate that in the spherulitic micelles formed directly after the solution of the cA peptide into various solvents, the peptide adopts a left-handed parallel  $\beta$ -helix type of structure, modeled accurately previously (Iconomidou et al., 2000), which, as a model of the cA peptide structure, has several attractive features as well. We propose here that the

transition from the spherulitic liquid crystalline phase to the mature fibrillar amyloid state involves a transformation of the left-handed parallel  $\beta$ -helix type of structure to the antiparallel  $\beta$ -sheet type of structure present in the mature fibrils of the amyloid state. This molecular conformational “switch” can easily be achieved by a transition of a type II  $\beta$ -turn (in the structure of the left-handed parallel  $\beta$ -helix) to a type II'  $\beta$ -turn (in the structure of the antiparallel  $\beta$ -pleated sheet) every six residues along the sequence of the cA peptide. Whether this is actually true remains to be seen by more refined experimental future work. If it is true, it will be the first case whereby a peptide capable to form amyloid fibrils may adopt two, well defined,  $\beta$ -sheet structures of a different kind. Apparently, nature, after millions of years of molecular evolution, has designed, in a rather unique way, these, dual-structure, amyloid-like chorion peptides to play an important functional role: to protect the oocyte and the developing embryo from a wide range of environmental hazards.

It is also clear that, the results of this study have important morphogenetic implications for silkworm chorion structure as well: silkworm chorion, a biological analogue of a cholesteric liquid crystal (Hamodrakas, 1992 and references therein) self-assembles from its constituent proteins a long distance away from the follicle cells which secrete these proteins on the surface of the oocyte. In this work, it has been shown conclusively that the cA peptide, a representative of the entire central domain of the A class of chorion proteins, that is a representative of 25% of the entire chorion mass approximately, self-assembles under a great variety of conditions into spherulitic liquid crystalline structures, obviously precursor substructures of silkworm chorion itself, which are transformed into amyloid-like fibrils constituting chorion. Thus, it appears that *in vitro* formation of such an important biological structure can be studied in detail. Since it might be argued that the peptide concentrations which lead to the liquid crystalline intermediates cannot occur *in vivo*, it should be mentioned that similar spherulitic structures are formed at very low (nM) concentrations of the cA peptide in the same solvents. These structures seem to retain their shape for a prolonged, not very well defined, period of time before their conversion into amyloid fibrils.

It remains also to be seen whether the results of this work can be generalized into other pathological cases involving amyloidoses and their, relevant in each case, proteins.

#### Acknowledgments

Financial support for this work was provided by the University of Athens. S.J.H. and V.A.I. acknowledge the help of the EMBL summer visitors program.

## References

- Benaki, D.C., Aggeli, A., Chryssikos, G.D., Yiannopoulos, Y.D., Kamitsos, E.I., Brumley, E., Case, S.T., Boden, N., Hamodrakas, S.J., 1998. Laser-Raman and FT-IR spectroscopic studies of peptide-analogues of silkworm chorion protein segments. *Int. J. Biol. Macromol.* 23, 49–59.
- Cai, S., Singh, B.R., 1999. Identification of  $\beta$ -turn and random coil amide III infrared bands for secondary structure estimation of proteins. *Biophys. Chem.* 80, 7–20.
- Carel, R.W., Gooptu, B., 1998. Conformational changes and disease-serpins, prions and Alzheimer's. *Curr. Opin. Struct. Biol.* 8, 799–809.
- Collaborative Computational Project, Number 4 The CCP4 Suite: Programs for Protein Crystallography 1994. *Acta Cryst.*, D50, 760–763.
- De Jongh, H.H.J., Goormaghtigh, E., Ruyschaert, J.M., 1996. The different molar absorptivities of the secondary structure types in the Amide I region: An attenuated total reflection infrared study on globular proteins. *Anal. Chem.* 242, 95–103.
- Dobson, C.M., 1999. Protein misfolding, evolution and disease. *Trends Biochem. Sci.* 24, 329–332.
- Guijarro, J.I., Sunde, M., Jones, J.A., Cambell, I.D., Dobson, C.M., 1998. Amyloid fibril formation by an SH3 domain. *Proc. Natl. Acad. Sci. USA* 95, 4224–4228.
- Hamodrakas, S.J., 1992. Molecular architecture of helicoidal proteinaceous eggshells. In: Case, S.T. (Ed.), *Results and Problems in Cell Differentiation*, vol. 19. Springer-Verlag, Berlin and Heidelberg, pp. 115–186 (Ch. 6).
- Hamodrakas, S.J., Etmektzoglou, T., Kafatos, F.C., 1985. Amino acid periodicities and their structural implications for the evolutionarily conservative central domain of some silkworm chorion proteins. *J. Mol. Biol.* 186, 583–589.
- Harris, P.I., Chapman, D., 1995. The conformational analysis of peptides using Fourier transform IR spectroscopy. *Biopolymers (Peptide Science)* 37, 251–263.
- Iconomidou, V.A., Vriend, G., Hamodrakas, S.J., 2000. Amyloids protect the silkworm oocyte and embryo. *FEBS Letters* 479, 141–145.
- Iconomidou, V.A., Chryssikos, G.D., Gionis, V., Vriend, G., Hoenger, A., Hamodrakas, S.J., 2001. Amyloid-like fibrils from an 18-residue peptide analogue of a part of the central domain of the B-family of silkworm chorion proteins. *FEBS Letters* 499, 268–273.
- Jackson, M., Mantsch, H.H., 1995. The use and misuse of FTIR spectroscopy in the determination of protein structure. *Critical Reviews in Biochemistry and Molecular Biology* 30 (2), 95–120.
- Kelly, J.W., 1996. Alternative conformations of amyloidogenic proteins govern their behavior. *Curr. Opin. Struct. Biol.* 6, 11–17.
- Kelly, J.W., 2000. Mechanisms of amyloidogenesis. *Nat. Struct. Biol.* 7, 824–826.
- Kenney, J.M., Knight, D., Wise, M.J., Vollrath, F., 2002. Amyloidogenic nature of spider silk. *Eur. J. Biochem.* 269, 4159–4163.
- Krimm, S., Bandekar, J., 1986. Vibrational spectroscopy and conformation of peptides, polypeptides, and proteins. *Adv. Prot. Chem.* 38, 181–386.
- Lekaniidou, R., Rodakis, G.C., Eickbush, T.H., Kafatos, F.C., 1986. Evolution of the silkworm chorion gene superfamily: gene families CA and CB. *Proc. Natl. Acad. Sci. USA* 83, 6514–6518.
- Lomakin, A., Chung, D.S., Benedek, G.B., Kirschner, D.A., Teplow, D.B., 1996. On the nucleation and growth of amyloid  $\beta$ -protein fibrils: Detection of nuclei and quantitation of rate constants. *Proc. Natl. Acad. Sci. USA* 93, 1125–1129.
- Parbhu, A., Lin, H., Thimm, J., Lal, R., 2002. Imaging real-time aggregation of amyloid beta protein (1–42) by atomic force microscopy. *Peptides* 23, 1265–1270.
- Regier, J.C., Kafatos, F.C., 1985. Molecular aspects of chorion formation. In: Gilbert, L.I. (Ed.), *Comprehensive Insect Biochemistry, Physiology and Pharmacology*, vol. I. Pergamon Press, Oxford and New York, pp. 113–151.
- Rochet, J.C., Lansbury Jr., P.T., 2000. Amyloid fibrillogenesis: themes and variations. *Curr. Opin. Struct. Biol.* 10, 60–68.
- Savitsky, A., Golay, M.J.E., 1964. Smoothing and differentiation of data by simplified least-squares procedures. *Anal. Chem.* 36, 1627–1639.
- Soto, C., 2001. Protein misfolding and disease; protein refolding and therapy. *FEBS Lett.* 498, 204–207.
- Sunde, M., Blake, C., 1997. The structure of amyloid fibrils by electron microscopy and X-ray diffraction. *Adv. Prot. Chem.* 50, 123–159.
- Sunde, M., Blake, C., 1998. From the globular to the fibrous state: protein structure and structural conversion in amyloid formation. *Quart. Rev. of Biophysics* 31 (1), 1–39.
- Surewicz, W.K., Mantsch, H.H., Chapman, D., 1993. Determination of protein secondary structure by Fourier transform infrared spectroscopy: A critical assessment. *Biochemistry* 32 (2), 389–394.
- Tan, S.Y., Pepys, M.B., 1994. Amyloidosis. *Histopathology* 25, 403–414.
- Walsh, D.M., Hartley, D.M., Kusumoto, Y., Fezoui, Y., Condron, M.M., Lomakin, A., Benedek, G.B., Selkoe, D.J., Teplow, D.B., 1999. Amyloid  $\beta$ -protein fibrillogenesis. Structure and biological activity of protofibrillar intermediates. *J. Biol. Chem.* 274, 25945–25952.
- Vollrath, F., Knight, D.P., 2001. Liquid crystalline spinning of spider silk. *Nature* 410, 541–548.
- Westlind-Danielsson, A., Arnerup, G., 2001. Spontaneous in vitro formation of supramolecular  $\beta$ -amyloid structures, “ $\beta$  amy balls”, by  $\beta$ -amyloid 1–40 peptide. *Biochemistry* 40, 14736–14743.
- Žerovnik, E., 2002. Amyloid fibril formation: Proposed mechanisms and relevance to conformational disease. *Eur. J. Biochem.* 269, 3362–3371.